Zuschriften

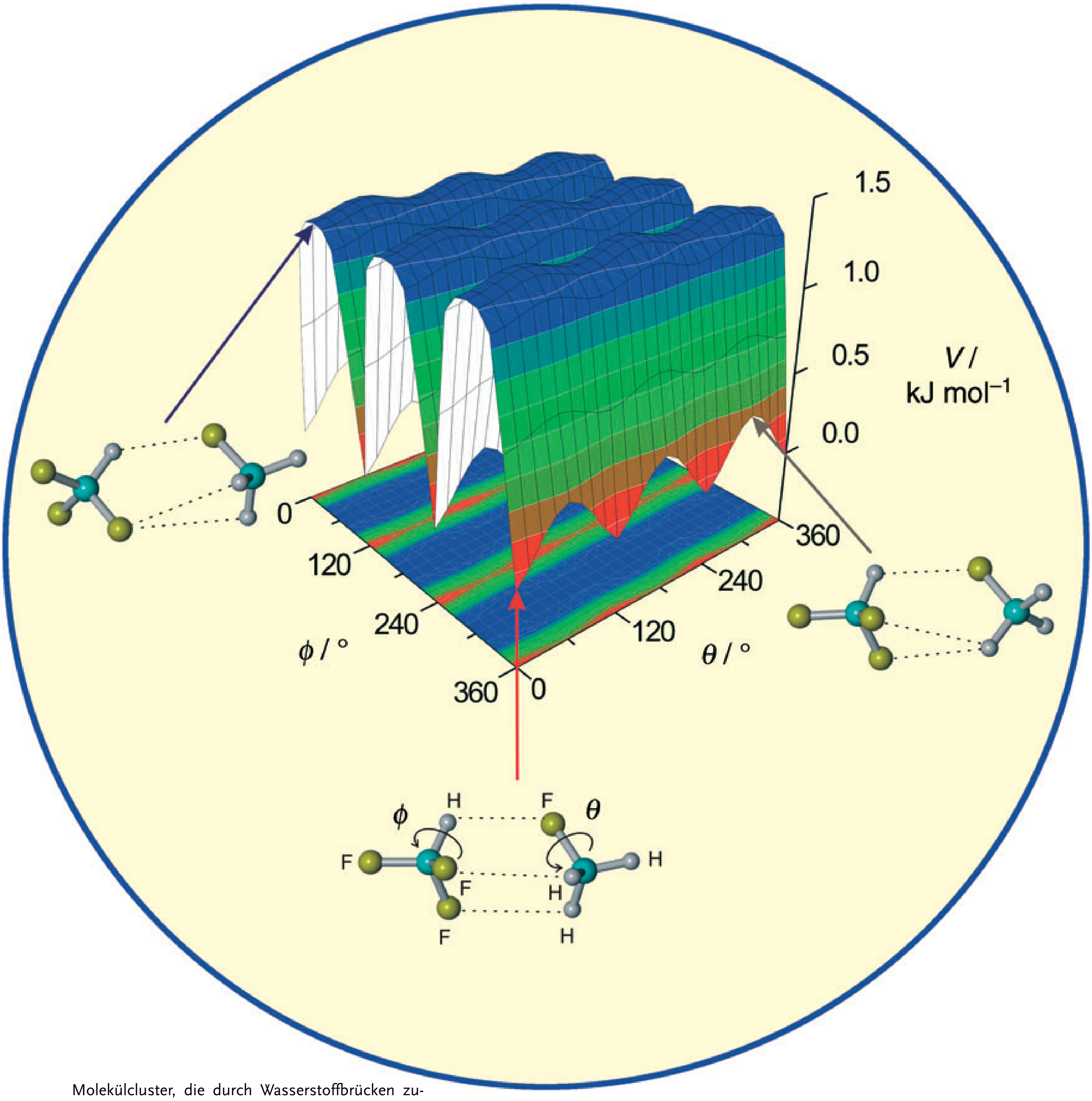

Molekülcluster, die durch Wasserstoffbrücken zusammengehalten werden, können hochdynamische Systeme sein, wie hier für einen Fluormethan-Trifluormethan-Komplex gezeigt ist: Die beiden Untereinheiten sind nicht starr fixiert, sondern in der Rotation um ihre Symmetrieachsen nahezu nicht eingeschränkt. Einzelheiten hierzu finden Sie in der Zuschrift von W. Caminati et al. auf den folgenden Seiten.

DOI: 10.1002/ange.200500775

Molecular Complexes

Weak CH···F Bridges and Internal Dynamics in the $CH_3F{\cdot}CHF_3$ Molecular Complex**

Walther Caminati, Juan C. López, José L. Alonso, and Jens-Uwe Grabow*

Herein, we report the effects of weak CH···F hydrogen bonds and dipole–dipole interaction energies on the conformation of the molecular complex fluoromethane–trifluoromethane and the internal dynamics of the two symmetric top subunits, which rotate almost freely with respect to each other.

The non-covalent interactions CH···F and CH···O, which play important roles in biological, atmospheric, and supramolecular chemistry, have been classified as weak hydrogen bonds (WHBs).[1] Studies on WHBs have been mainly performed by X-ray diffraction[2] and, to a lesser extent, by IR spectroscopy on solutions of rare gases.[3] The experimental data on WHB obtained from investigations in the solid or solution states are contaminated by other intermolecular interactions that take place in condensed phases and do not give information on the internal dynamics of the subunits held together by these interactions.

The few rotationally resolved investigations of molecular adducts in which the monomers are held together by CH···F and CH···O WHBs have shown the specificity and directionality of these interactions.[4–9] For example, the dimer of difluoromethane is stabilized only by CH···F bridges[4] and several theoretical investigations have been reported on this type of interaction.[10–12]

The heterodimer fluoromethane–trifluoromethane ($CH_3F{\cdot}CHF_3$) is also expected to contain only CH···F linkages, and an investigation of this dimer is of particular interest to assess the relative weights of the WHBs and dipole–dipole interaction energies. In Figure 1 two plausible conformations of $CH_3F{\cdot}CHF_3$ (A and B) are shown in which three WHBs stabilize the two subunits. In A the three hydrogen s orbitals in CH_3F can probably better overlap with the three fluorine p orbitals of the opposing molecule, but B has a more favorable electrostatic potential energy from the dipole–dipole interaction, with the two dipole moments almost antiparallel to each other. To elucidate the balance between these two stabilization mechanisms, we studied the rotational spectrum of $CH_3F{\cdot}CHF_3$ isolated in the interaction-free matrix of a supersonic jet by employing Fourier-transform microwave spectroscopy (see Experimental Section for details). We could assign only the spectrum of species B: 32, 12, and 11 rotational transitions (see Supporting Information) have been measured for the normal, $CH_3F{\cdot}^{13}CHF_3$, and $^{13}CH_3F{\cdot}CHF_3$ isotopomers, respectively. At an overall point group symmetry of C_s, the molecular complex has two inequivalent internal rotors of C_{3v} symmetry. By taking the feasible large amplitude motions into account within the permutation-inversion (PI) group theory formalism,[13] the appropriate molecular symmetry (MS) group will be G_{18} and the torsional wavefunctions can accordingly be symmetry-classified as A_1, E_1, E_2, E_3, and E_4.[14] All measured transitions were split into a non- and a doubly degenerate (designated A_1 and E_1, respectively) component line as a result of the internal rotation of the CHF_3 group around its symmetry axis. The three other components, E_2, E_3, and E_4, which arise from the internal rotation of the CH_3F group and the interaction between both groups, were not observed. For a very low tunneling barrier, the corresponding splittings are predicted to be very large and thus difficult to locate. The combined analysis of the rotational transition frequencies for the A_1 and E_1 states of the internal rotations of the CHF_3 group[15] yielded the spectroscopic constants shown in Table 1. The internal rotation parameters[16] included therein are: 1) I_α, the moment of inertia of the CHF_3 top, 2) $\measuredangle\,(a,i)$, the angle between the internal rotation axis of the CHF_3 top and the principal axis of inertia a of the complex, and 3) V_3, the barrier to internal rotation of the CHF_3 top. For the two less abundant isotopomers the results were similar; the larger standard errors are a result of the smaller experimental data set. The effective moment of inertia determined from the A_1–E_1 splitting pattern for an internal rotor (see Table 2) in

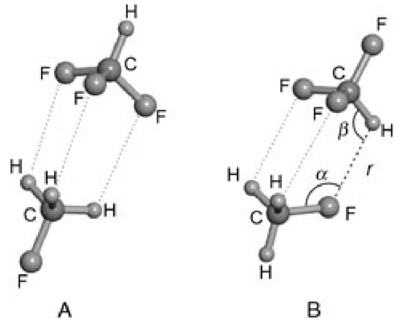

Figure 1. Plausible conformations (A and B) of $CH_3F{\cdot}CHF_3$ highlighting the structural parameters (r, α, and β).

---

[*] Prof. Dr. W. Caminati
Dipartimento di Chimica "G. Ciamician" dell'Università
Via Selmi 2, 40126 Bologna (Italy)
Fax: (+39) 051-209-9456
E-mail: walther.caminati@unibo.it
Prof. Dr. J. C. López, Prof. Dr. J. L. Alonso
Departamento de Química-Física y Química-Inorgánica
Facultad de Ciencias
Universidad de Valladolid
47005 Valladolid (Spain)
Priv.-Doz. Dr. J.-U. Grabow
Institut für Physikalische Chemie und Elektrochemie
Lehrgebiet A
Callinstrasse 3–3 a, 30167 Hannover (Germany)

[**] We would like to thank the Ministers of Education of Italy and Spain, and the Deutscher Akademischer Austauschdienst (DAAD) of Germany for the support given through three bilateral programs: 1) Italy–Spain (Azione Integrata It294-2001, Acción Integrada HI-2000-0092); 2) Germany–Italy (PPP D/0231300 and Progetto VIGONI 2003 21-2002); 3) Spain–Germany (Acciones Integradas HA-2002-0014 and PPP D/0246239). W.C. thanks the University of Bologna, and J.C.L. and J.L.A. thank the Dirección General de Investigación—Ministerio de Ciencia y Tecnología the Junta de Castilla y León—for financial support.

Table 1: Spectroscopic constants for adduct $CH_3F{\cdot}CHF_3$.[a]

Parameter	$CH_3F{\cdot}CHF_3$	$CH_3F{\cdot}^{13}CHF_3$	$^{13}CH_3F{\cdot}CHF_3$
A [MHz]	6451.696(2)	6456(5)	6440(2)
B [MHz]	1459.976(6)	1456.23(2)	1430.48(1)
C [MHz]	1413.440(6)	1410.10(2)	1386.47(1)
D_J [kHz]	2.740(3)	2.720(7)	2.668(3)
D_{JK} [kHz]	53.44(2)	52.2(5)	51.2(2)
D_K [kHz]	16.3(3)	16.3[b]	16.3[b]
d_J [kHz]	0.222(2)	0.219(5)	0.204(2)
d_K [kHz]	1.4(9)	1.4[b]	1.4[b]
I_α [u Å^2]	86.0(3)	89(3)	86(2)
∢(a,i) [°][c]	51.4(1)	53(2)	50.6(8)
V_3 [kJ mol^{-1}]	0.840(5)	0.80(3)	0.88(2)
N[d]	64	24	22
σ [kHz][e]	3.2	4.1	1.5
P_{bb} [u Å^2]	44.865(1)[f]	44.82(4)	44.85(2)

[a] A_1 and E_1 states of the internal rotation; I^r representation of Watson's *S*-reduced Hamiltonian.[15]. Standard errors in parentheses are given in units of the last digit.[b] Parameters were fixed to those of the normal species. [c] ∢(a,i) is the angle between the inertial axes *a* and the internal rotation axis *I*; ∢(b,i) is the complement of ∢(a,i) at 90°, while ∢(c,i) is 90° from the symmetry axis. [d] Number of transition frequencies in the fit. [e] Root-mean-square deviation of the fit. [f] Smaller than the sum (46.17 u Å^2) of the P_{bb} values of isolated CHF_3 and CH_3F (44.62 and 1.55 u Å^2, respectively).

Table 2: Comparison of the internal rotation parameters for the CF_3 and CH_3 internal rotors of $CH_3F{\cdot}CHF_3$.

Internal rotor	CF_3	CH_3
I_α [u Å^2]	85.0	3.20
V_3 [kJ mol^{-1}]	0.840	0.36
s	67.92	2.5
Δ_{AE} [MHz][a]	2.6×10^{-1}	1.2×10^{5}
N_{levels}[b]	12	2

[a] Energy spacing between the A_1 and E_1 or E_2 sublevels, that is, $W(E_1)-W(A_1)$ and $W(E_2)-W(A_1)$, respectively, of the vibrational ground state. [b] Number of bound levels below the corresponding V_3 barrier.

$CH_3F{\cdot}CHF_3$ is only slightly smaller than the value of 89.23(2) u Å^2 for isolated CHF_3.[17] This result indicates that the motion responsible for the A_1–E_1 spectral separations is essentially the rotation of the CHF_3 group around an axis close to its C_3 symmetry axis.

The A_1–E_2 torsional splitting was deduced also for the internal rotation of the lighter CH_3F group. This splitting is related to the unexpectedly low value of the planar moment of inertia, P_{bb}, of the complex. The planar moments of inertia, defined as $P_{aa} = 1/2\,(-I_{aa}+I_{bb}+I_{cc})$, and cyclic permutations give the extensions of the molecular system in the directions of the considered principal axis. For the $CH_3F{\cdot}CHF_3$ complex the value of P_{bb} should correspond to the sum of the values of P_{bb} for the two isolated symmetric tops (1.55 and 44.62 u Å^2),[17,18] that is, 46.17 u Å^2. This is the case, for example, for oxirane·CHF_3,[6] for which P_{bb} (63.86 u Å^2) is almost exactly the sum of the P_{aa} value of oxirane and the P_{bb} value of CHF_3 (19.43 and 44.62 u Å^2, respectively). In $CH_3F{\cdot}CHF_3$, P_{bb} is 44.69 u Å^2, which is lower by 1.48 u Å^2 than the sum value (46.17 u Å^2). Such an unusually low value of P_{bb} is indicative of an exceptionally low V_3 barrier to the internal rotation of the methyl group. In fact, rotational constants are effective quantities that include the "pseudo" contributions due to the internal rotation of the methyl group, according to Equation (1),[19] in which A_r, B_r, and C_r are the "rigid" rotational constants in the limit of the very high barrier; $W_{00}^{(n)}$ are Hersbach's barrier-dependent perturbation sums relative to the A sublevels of the ground state;[20] F is the reduced constant of the motion; $\rho_g = \lambda_g I_\alpha / I_g$.

$$\begin{aligned} A_{00} &= A_r + W_{00}^{(2)} F \rho_a^2 \\ B_{00} &= B_r \\ C_{00} &= C_r + W_{00}^{(2)} F \rho_c^2 \end{aligned} \qquad (1)$$

The experimentally determined value of P_{bb} is obtained at $V_3 = 30$ cm^{-1}. As the curve V_3 versus P_{bb} is very steep at that point, we can set an estimated error of 10 cm^{-1}. The parameters relevant to the internal rotations of CH_3F and CHF_3 are compared in Table 2. Although the two V_3 barriers are relatively similar, the reduced barriers *s*, which contain both potential- and kinetic-energy factors, are very different from each other. Correspondingly, the A_1–E_1 and A_1–E_2 splittings, that is, the Δ_{AE} energy spacings between the A_1 and E_1 or E_2 sublevels, respectively, of the vibrational ground state, differ by six orders of magnitude.

For several molecular complexes, it has been possible to estimate the force constant (k_s) of the stretching motions between the two moieties that lead to dissociation, by using approximated Equation (2),[21] in which μ, R_{CM}, B, C, and D_J are the reduced mass, the distance between the monomer centers of mass, the rotational constants, and the first-order centrifugal distortion constant, respectively, of the adduct, and h is Planck's constant. However, in the case of $CH_3F{\cdot}CHF_3$, the effective parameter D_J contains contributions from one of the large amplitude motions, that is, the internal rotation of the CH_3F group. These contributions can be calculated with Equation (3).[22]

$$k_s = 16\pi^4 (\mu R_{CM})^2 [4B^4 + 4C^4 - (B-C)^2 (B+C)^2]/(h D_J) \qquad (2)$$

$$D_J = -1/2\,(\rho_b^4 + \rho_c^4)\, W_{00}^{(4)} F \qquad (3)$$

The estimated correction (0.029 kHz) to the effective value in Table 1 is very small. Thus, by using the value of 2.711 kHz in Equation (2), a value $k_s = 5.2$ N m^{-1}, which corresponds to a harmonic stretching frequency of 62 cm^{-1}, was obtained. The dissociation energy (E_D) has been evaluated to be 5.3 kJ mol^{-1} by assuming a Lennard–Jones potential function and using the approximated equation[23] $E_D = 1/72\, k_s R_{CM}^2$. Such a dissociation energy corresponds to a binding energy of 1.8 kJ mol^{-1} for each C–H···F linkage. This value is very similar to that found for the dimer of difluoromethane, which also displays three C–F···H–C interactions.[4]

If we assume the geometries of isolated CHF_3[17] and CH_3F[18] to remain unaltered in the adduct, we have sufficient experimental data to obtain a plausible r_0 structure, that is, to determine the three parameters r, α, and β shown in Figure 1. First, we calculated the rigid values of the rotational constants by applying the CH_3 corrections indicated in Equation (1) to the effectively determined rotational constants. Then we fitted the nine available rotational constants to obtain the three parameters. In the fit, we allowed these parameters to change, with respect to the ab initio values, at "confidence intervals" of 0.01 Å for the bond distance and at 2° for the two angles, respectively, according to the diagnostic least-squares procedure described by Curl.[24] The three parameters, r, α, and β, are reported in Table 3, together with the derived distance of the other hydrogen bonds. The substitution coordinates[25] of the carbon atoms of the CH_3F and CHF_3 subunits (see Table 3 footnotes) allow the C–C distances, which are also listed in Table 3, to be determined.

Table 3: Relevant structural parameters of $CH_3F{\cdot}CHF_3$ (see Figure 1).

r_0 parameters	r_0[a]	r_s[b]	ab initio[c]
$r(F_{CH_3F}\cdots H_{CHF_3})$ [Å][a]	2.427(10)	–	2.405
α [°][a]	124.1(3)	–	122.3
β [°][a]	115.5(3)	–	109.9
$r(F_{CHF_3}\cdots H_{CH_3F})$ [Å][d]	3.052(15)	–	2.842
$r(C_{CH_3F}\cdots C_{CHF_3})$ [Å][d]	3.645	3.60(2)[e]	3.522

[a] $r(F_{CH_3F}\cdots H_{CHF_3})$, which coincides with r of Figure 1, α, and β are the fitted parameters. The remaining parameters have been derived from the obtained partial r_0 geometry. [b] From the substitution coordinates of CH_3F and CHF_3 carbon atoms. [c] Computed values at MP2/6-311++G(2df,2p) level. [d] Derived parameter. [e] C⋯C distance between the carbon atoms of CH_3F and CHF_3. From r_s coordinates of C_{CHF_3} [$|a|=0.84(6)$; $|c|=0.43(4)$ Å] and of C_{CH_3F} [$|a|=2.619(7)$; $|c|=0.57(3)$ Å]. $|b|$ is fixed to 0 because imaginary.

Ab initio computations at the MP2/6-311++G(2df,2p) level[26] at different points of the $CH_3F{\cdot}CHF_3$ potential-energy surface have been performed to investigate the conformational behavior of the dimer. Conformer B is predicted to be the global minimum. Some of the calculated structural parameters for this conformer are compared to the experimental values in Table 3. The counterpoise (CP)-corrected dissociation energy for this conformer is calculated to be 10.0 kJ mol^{-1}, which is higher than that determined from the centrifugal distortion. Conformer A is predicted to be also a stable minimum, some 714 cm^{-1} (619 cm^{-1} after CP corrections) higher in energy than species B.

Other plausible conformers shown in Figure 2 were also considered. However, at this level of theory these conformers are predicted to be transition configurations with one negative frequency. Figure 3 shows the calculated potential-energy curves that describe the internal rotation of CHF_3 and CH_3F around their local C_3 axes. As indicated, the measured V_3 values thus give the experimental energies of configurations C and D with respect to B. They are in good agreement with the ab initio values, although the results of ab initio calculations lead us to anticipate that the shape of the potential-energy surface is more complicated.

In summary, we have shown how rotational spectroscopy can supply detailed information on the chemical features of weak hydrogen bonds and provide insight on the internal dynamics of the unit constituents of molecular complexes with unrivaled precision. In the case of $CH_3F{\cdot}CHF_3$ studied here, the CH_3F moiety "sees" CHF_3 in a well-defined position, while the CHF_3 unit "sees" CH_3F as a "cone".

Experimental Section

Commercial samples of CH_3F (Aldrich) and CHF_3 (Linde gas) were used without further purification. The spectra of the isotopic ^{13}C-containing species were measured in natural abundance.

The rotational spectrum in the 6–18.5 GHz frequency region was measured using a coaxially oriented beam-resonator arrangement-(COBRA)-type[27] pulsed supersonic jet Fourier-transform microwave (FT-MW) spectrometer,[28] as described elsewhere[29] and recently updated with the FTMW++ set of programs.[30]

A gaseous mixture of CH_3F (1 %) and CHF_3 (1 %) in He at a total pressure of 2.0 bar was expanded through the solenoid valve (General Valve, Series 9, nozzle diameter 0.5 mm) into the Fabry–Pérot cavity. The spectral line positions were determined after Fourier transformation of the 8000-data-point time-domain signal, recorded at intervals of 100 ns. Each rotational transition is split by the Doppler effect as a result of the coaxial arrangement of the supersonic jet and resonator axes in the COBRA-FTMW spectrometer. The rest frequency is calculated as the arithmetic mean of the frequencies of the Doppler components. The estimated accuracy of frequency measurements is greater than 3 kHz. Lines separated by more than 7 kHz are resolvable.

Received: March 2, 2005

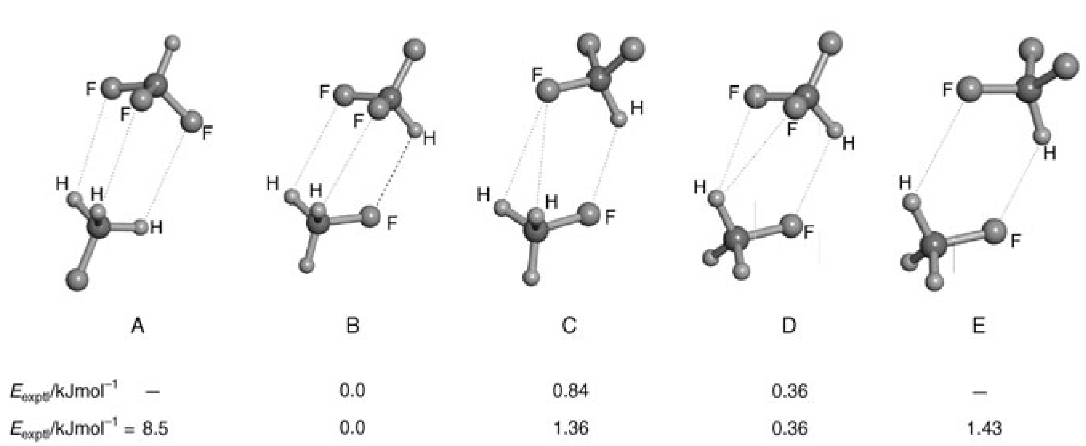

Figure 2. Relative energies of configurations A and C–E with respect to the observed conformer B. Configurations C–E are transition states (saddle points), not stable minima. In particular, the energies of C and D correspond to the two V_3 barriers.

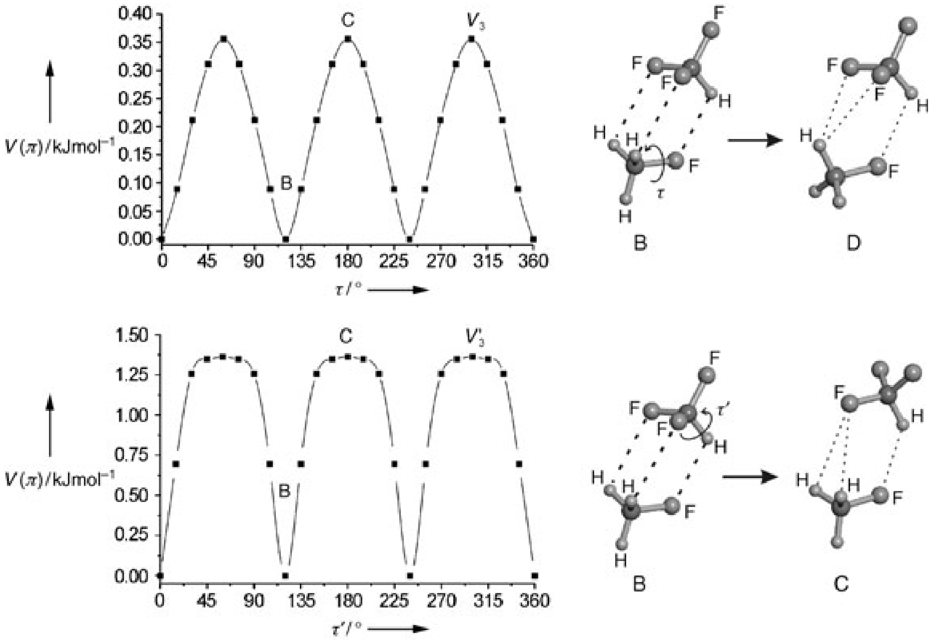

Figure 3. Local potential-energy curves for the two large amplitude tunneling motions in $CH_3F\cdot CHF_3$.

Keywords: halomethanes · hydrogen bonds · molecular complexes · molecular dynamics · rotational spectroscopy

---

[1] "The Weak Hydrogen Bond in Structural Chemistry and Biology": *IUCr Monographs on Crystallography*, *Vol. IX* (Eds.: G. R. Desiraju, T. Steiner), Oxford University Press, Oxford, **2001**.

[2] T. Steiner, *Angew. Chem.* **2002**, *114*, 50; *Angew. Chem. Int. Ed.* **2002**, *41*, 48.

[3] S. N. Delanoye, W. A. Herrebout, B. J. van der Veken, *J. Am. Chem. Soc.* **2002**, *124*, 11854.

[4] a) W. Caminati, S. Melandri, P. Moreschini, P. G. Favero, *Angew. Chem.* **1999**, *111*, 3105; *Angew. Chem. Int. Ed.* **1999**, *38*, 2924; b) S. Blanco, J. C. López, A. Lesarri, J. L. Alonso, *J. Mol. Struct.* **2002**, *612*, 255.

[5] Y. Tatamitani, B. Liu, J. Shimada, T. Ogata, P. Ottaviani, A. Maris, W. Caminati, J. L. Alonso, *J. Am. Chem. Soc.* **2002**, *124*, 2739.

[6] J. L. Alonso, S. Antolínez, S. Blanco, A. Lesarri, J. C. López, W. Caminati, *J. Am. Chem. Soc.* **2004**, *126*, 3244.

[7] Y. Tatamitami, T. Ogata, *J. Mol. Spectrosc.* **2003**, *222*, 102.

[8] S. Blanco, J. C. López, A. Lesarri, W. Caminati, J. L. Alonso, *ChemPhysChem* **2004**, *5*, 1779.

[9] G. C. Cole, A. C. Legon, *Chem. Phys. Lett.* **2003**, *369*, 31.

[10] E. Espinosa, I. Alkorta, J. Elguero, E. Molins, *J. Chem. Phys.* **2002**, *117*, 5529.

[11] E. Kryachko, S. Scheiner, *J. Phys. Chem. A* **2004**, *108*, 2527.

[12] E. Ebrahimi, H. Roohi, S. M. Habibi, *J. Mol. Struct. (Theochem)* **2004**, *684*, 87.

[13] H. C. Longuet Higgins, *Mol. Phys.* **1963**, *6*, 445.

[14] H. Dreizler, *Z. Naturforsch.* **1961**, *16*, 1354. For a typical example, see: J. Sheridan, W. Bossert, A. Bauder, *J. Mol. Spectrosc.* **1980**, *80*, 1.

[15] H. Hartwig, H. Dreizler, *Z. Naturforsch. A* **1996**, *51*, 923, according to the I^r representation of Watson's *S*-reduced Hamiltonian: J. K. G. Watson in *Vibrational Spectra and Structure*, *Vol. 6* (Ed.: J. R. Durig), Elsevier, New York, **1977**, pp. 1–89.

[16] R. C. Woods, *J. Mol. Spectrosc.* **1966**, *21*, 4.

[17] Y. Kawashima, A. P. Cox, *J. Mol. Spectrosc.* **1978**, *72*, 423.

[18] R. Bocquet, W. D. Chen, D. Papousek, G. Wlodarczak, J. Demaison, *J. Mol. Spectrosc.* **1994**, *164*, 456.

[19] D. R. Herschbach, J. D. Swalen, *J. Chem. Phys.* **1958**, *29*, 761.

[20] D. R. Herschbach, *J. Chem. Phys.* **1959**, *31*, 91.

[21] a) D. J. Millen, *Can. J. Chem.* **1985**, *63*, 1477; b) W. G. Read, E. J. Campbell, G. Henderson, *J. Chem. Phys.* **1983**, *78*, 3501.

[22] W. Caminati, *J. Mol. Spectrosc.* **1982**, *90*, 315.

[23] R. P. A. Bettens, R. M. Spycher, A. Bauder, *Mol. Phys.* **1995**, *86*, 487.

[24] R. F. Curl, *J. Comput. Phys.* **1957**, *27*, 343.

[25] J. Kraitchman, *Am. J. Phys.* **1953**, *21*, 17.

[26] Gaussian 03 (Revision B.04), M. J. Frisch, G. W. Trucks, H. B. Schlegel, G. E. Scuseria, M. A. Robb, J. R. Cheeseman, J. A. Montgomery, Jr., T. Vreven, K. N. Kudin, J. C. Burant, J. M. Millam, S. S. Iyengar, J. Tomasi, V. Barone, B. Mennucci, M. Cossi, G. Scalmani, N. Rega, G. A. Petersson, H. Nakatsuji, M. Hada, M. Ehara, K. Toyota, R. Fukuda, J. Hasegawa, M. Ishida, T. Nakajima, Y. Honda, O. Kitao, H. Nakai, M. Klene, X. Li, J. E. Knox, H. P. Hratchian, J. B. Cross, C. Adamo, J. Jaramillo, R. Gomperts, R. E. Stratmann, O. Yazyev, A. J. Austin, R. Cammi, C. Pomelli, J. W. Ochterski, P. Y. Ayala, K. Morokuma, G. A. Voth, P. Salvador, J. J. Dannenberg, V. G. Zakrzewski, S. Dapprich, A. D. Daniels, M. C. Strain, O. Farkas, D. K. Malick, A. D. Rabuck, K. Raghavachari, J. B. Foresman, J. V. Ortiz, Q. Cui, A. G. Baboul, S. Clifford, J. Cioslowski, B. B. Stefanov, G. Liu, A. Liashenko, P. Piskorz, I. Komaromi, R. L. Martin, D. J. Fox, T. Keith, M. A. Al-Laham, C. Y. Peng, A. Nanayakkara, M. Challacombe, P. M. W. Gill, B. Johnson, W. Chen, M. W. Wong, C. Gonzalez, J. A. Pople, Gaussian, Inc., Pittsburgh, PA, **2003**.

[27] J.-U. Grabow, W. Stahl, *Z. Naturforsch. A* **1990**, *45*, 1043; J.-U. Grabow, doctoral thesis, Christian-Albrechts-Universität zu Kiel, Kiel, **1992**; J.-U. Grabow, W. Stahl, H. Dreizler, *Rev. Sci. Instrum.* **1996**, *67*, 4072.

[28] T. J. Balle, W. H. Flygare, *Rev. Sci. Instrum.* **1981**, *52*, 33.

[29] W. Caminati, A. Millemaggi, J. L. Alonso, A. Lesarri, J. C. Lopez, S. Mata, *Chem. Phys. Lett.* **2004**, *392*, 1.

[30] J.-U. Grabow, *56th Ohio State University International Conference on Molecular Spectroscopy*, MG01, Columbus **2001**; J.-U. Grabow, Habilitationsschrift, Universität Hannover, Hannover **2004**; http://www.pci.uni-hannover.de/~lgpca/spectroscopy/ftmw.